Signaling and Regulation

Molecular Cancer Research

Long-Range Epigenetic Silencing Associates with Deregulation of Ikaros Targets in Colorectal Cancer Cells

Biola M. Javierre[1], Javier Rodriguez-Ubreva[1], Fatima Al-Shahrour[3,4], Marina Corominas[1], Osvaldo Graña[5], Laura Ciudad[1], Xabier Agirre[6], David G. Pisano[5], Alfonso Valencia[5], Jose Roman-Gomez[7], Maria Jose Calasanz[8], Felipe Prosper[6], Manel Esteller[2], Rogelio Gonzalez-Sarmiento[9], and Esteban Ballestar[1]

Abstract

Transcription factors are common targets of epigenetic inactivation in human cancer. Promoter hypermethylation and subsequent silencing of transcription factors can lead to further deregulation of their targets. In this study, we explored the potential epigenetic deregulation in cancer of *Ikaros* family genes, which code for essential transcription factors in cell differentiation and exhibit genetic defects in hematologic neoplasias. Unexpectedly, our analysis revealed that *Ikaros* undergoes very specific promoter hypermethylation in colorectal cancer, including in all the cell lines studied and around 64% of primary colorectal adenocarcinomas, with increasing proportions in advanced Duke's stages. *Ikaros* hypermethylation occurred in the context of a novel long-range epigenetic silencing (LRES) region. Reintroduction of Ikaros in colorectal cancer cells, ChIP-chip analysis, and validation in primary samples led us to identify a number of direct targets that are possibly related with colorectal cancer progression. Our results not only provide the first evidence that LRES can have functional specific effects in cancer but also identify several deregulated Ikaros targets that may contribute to progression in colorectal adenocarcinoma. *Mol Cancer Res; 9(8); 1139–51. ©2011 AACR.*

Introduction

Epigenetic dysregulation of gene silencing plays a causal role in cancer development and progression. One of the most common epigenetic alterations in cancer results from *de novo* DNA methylation of promoter CpG islands (1). Initial studies using candidate gene approaches showed that many tumor suppressor genes undergo aberrant hypermethylation in cancer and that these events occur in a tumor type–specific manner (2, 3). More recently, the use of genome-wide screening techniques has shown that hypermethylation in cancer occurs in different groups of genes, including those encoding transcription factors involved in tissue-specific differentiation and development (4). Various chromatin factors that are important in maintaining a normal silenced transcription status in a cell type–specific manner are now known to play a pivotal role in determining which genes become hypermethylated in cancer, when aberrantly used by the DNA methylation machinery. For instance, polycomb-induced H3K27 trimethylation, which is involved in gene silencing during development, associates with DNA hypermethylation in cancer (5, 6). More recently, genome-wide surveys have uncovered other mechanisms. For instance, Frigola and colleagues found coordinated hypermethylation of 12 closely located CpG islands in colorectal cancer (7) and recent data suggest that concurrent hypermethylation of adjacent CpG islands and associated gene repression, also known as long-range epigenetic silencing (LRES), may be a more common phenomenon in cancer than previously recognized (8–11).

It is inherently interesting to investigate the functional consequences of the epigenetic inactivation of particular genes. Transcription factor–encoding genes often undergo cancer-associated hypermethylation and their silencing can result in further deregulation of their target genes. In this study, we focused on the epigenetic deregulation in cancer of the Ikaros family of transcription factors, which are essential regulators of cell differentiation (12). The family

Authors' Affiliations: [1]Chromatin and Disease Group and [2]Cancer Epigenetics Group, Cancer Epigenetics and Biology Programme (PEBC), Bellvitge Biomedical Research Institute (IDIBELL), L'Hospitalet de Llobregat, Barcelona, Spain; [3]Broad Institute, Cambridge; [4]Hematology Division, Brigham and Women's Hospital, Harvard Medical School, Brookline, Massachusetts; [5]Bioinformatics Unit and Structural Biology and Biocomputing Programme, Spanish National Cancer Centre, Madrid; [6]Hematology Department and Area of Cell Therapy, Clínica Universidad de Navarra, Foundation for Applied Medical Research, [7]Hematology Department, Reina Sofia Hospital, Cordoba; [8]Department of Genetics, School of Sciences, University of Navarra, Pamplona; and [9]Molecular Medicine Unit-Department of Medicine, Center for Cancer Research, University of Salamanca, Salamanca, Spain

Note: Supplementary data for this article are available at Molecular Cancer Research Online (http://mcr.aacrjournals.org/).

Corresponding Author: Esteban Ballestar, Chromatin and Disease Group, Cancer Epigenetics and Biology Programme, Bellvitge Biomedical Research Institute, Avda. Gran Via 199-203, 08908 L'Hospitalet de Llobregat, Barcelona 08907, Spain. Phone: 34-932607133; Fax: 34-932607219; E-mail: eballestar@idibell.org

doi: 10.1158/1541-7786.MCR-10-0515

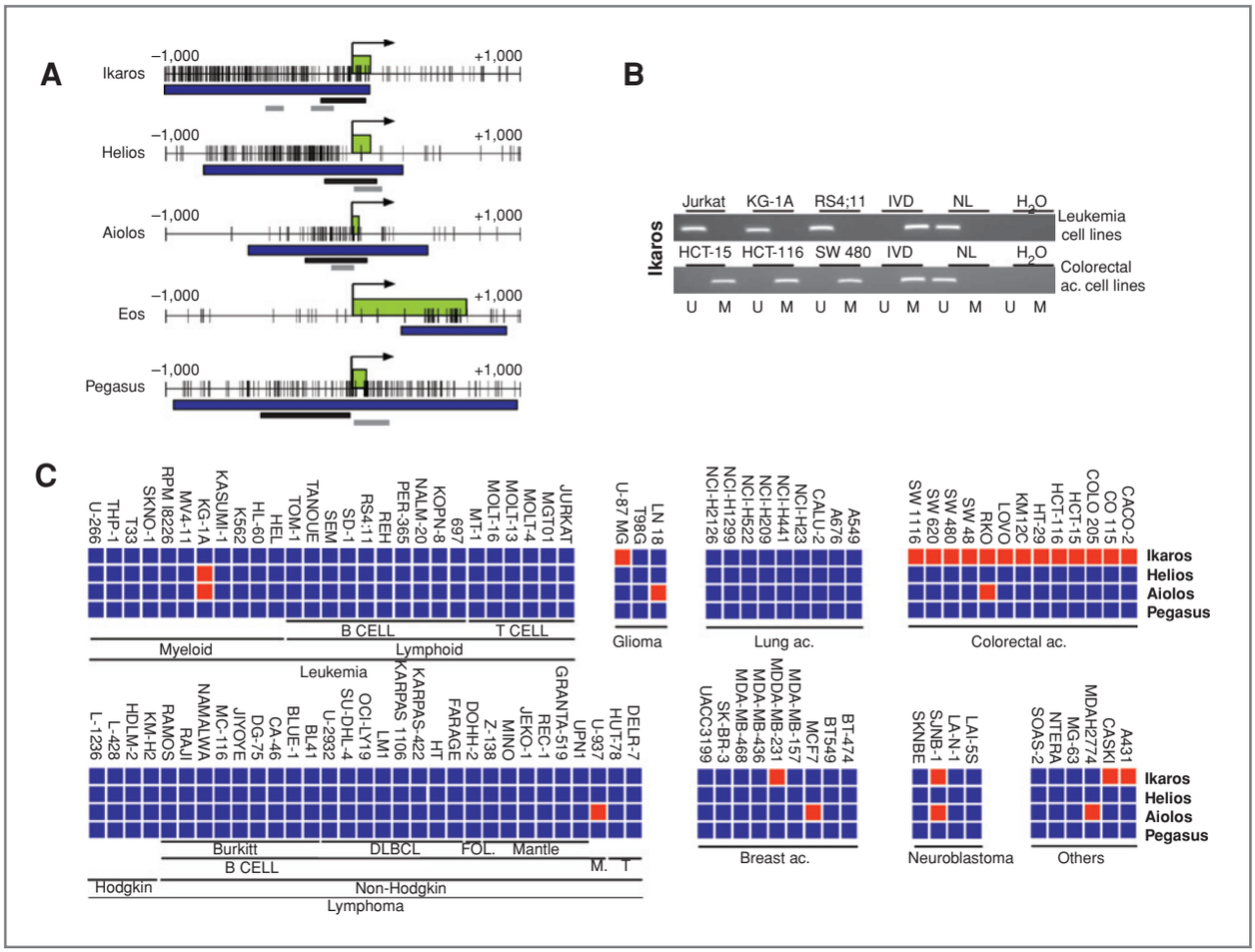

Figure 1. *Ikaros* displays a specific pattern of hypermethylation in colorectal adenocarcinoma. A, diagram depicting CpG distribution in all *Ikaros* family genes between −1,000 bp to +1,000 bp relative to the TSS (indicated by an arrow). CpG sites are represented as vertical black lines and CpG islands are highlighted by horizontal blue bars. Promoter regions analyzed by MSP and BS are respectively indicated by gray and black bars. B, MSP analysis of *Ikaros* promoter CpG island in leukemia and colorectal cancer (ac) cell lines. The presence of a PCR band under lanes M or U indicates methylated or unmethylated, respectively. *In vitro* methylated DNA (IVD) is used as a positive control. C, methylation analysis of the 4 promoter CpG island–containing *Ikaros* family genes in a panel of hematologic neoplasia cell lines and additional cell lines (colorectal, lung and breast adenocarcinomas, neuroblastomas, and gliomas). Blue and red squares respectively indicate unmethylated and methylated status.

consists of five members (Ikaros, Helios, Aiolos, Eos, and Pegasus), which arose from multiple duplication events. Ikaros family members share similarities at several levels. For instance, Ikaros, Helios, Aiolos, and Eos have identical splicing patterns that generate multiple isoforms with similar combinations of exons. Another similarity among *Ikaros* family genes involves their surrounding sequences, where the colocalization of homologous neighboring genes is preserved. In parallel, *Ikaros* family genes are expressed in overlapping cell types, suggesting the conservation of transcription factors and epigenetic mechanisms that regulate their expression. These factors are characteristic of the hematopoietic system and are specifically expressed at different stages of the lymphoid branch. Recent studies highlight the importance of genetic alterations undergone by Ikaros family members in various hematologic neoplasias (13–15).

We sought to establish whether the *Ikaros* family genes were epigenetically deregulated in human cancer. We observed an almost complete absence of hypermethylation in most tumor types including hematologic neoplasias. However, for *Ikaros*, we found promoter hypermethylation in all colorectal cancer cell lines studied and in more than 60% of primary colorectal cancer samples. Interestingly, we found that Ikaros is embedded in an LRES region that undergoes additional silencing in colorectal adenocarcinoma. ChIP-chip analysis following reintroduction of Ikaros allowed us to identify a number of Ikaros targets in colorectal cancer with a potential role in its development and progression. Our results are of 2-fold interest: first, LRES has specific functional effects in cancer through deregulation of Ikaros gene targets; second, we have defined a Duke's stage–associated epigenetic change for *Ikaros* in colorectal adenocarcinoma that involves deregulation of a

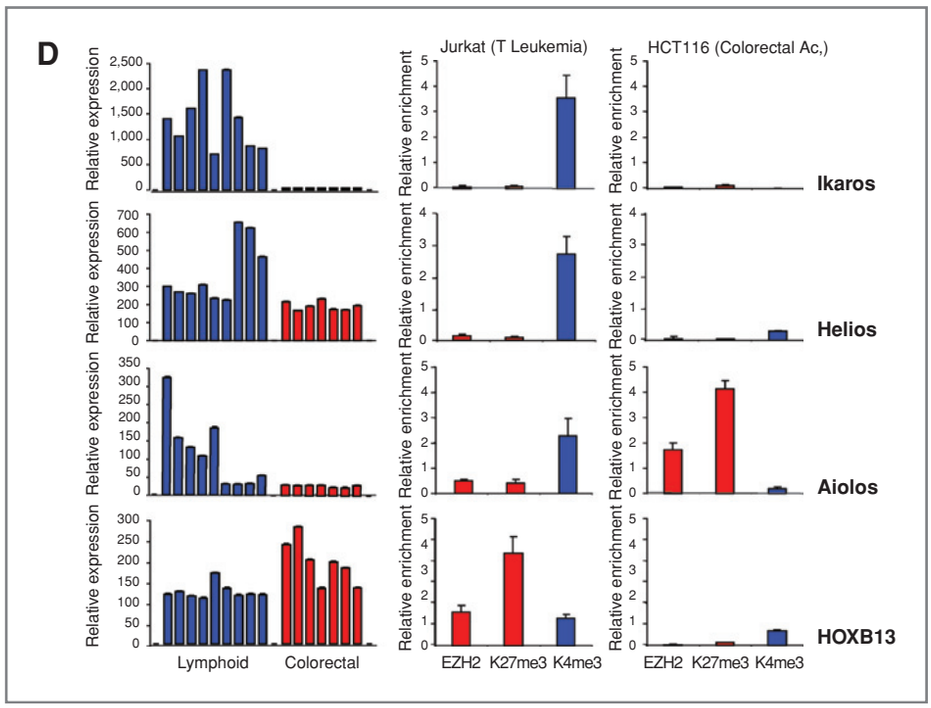

Figure 1. (*Continued*) D, expression and ChIP data for Ikaros, Helios, Aiolos, and HOXB13 in the colorectal and T lymphoid system. Expression data (left) were obtained from the Oncomine Wooster database and contain a variety of lymphoid neoplasias (DG-75, Jiyoye, MC-116, NAMALWA, RAJI, MOLT-4, MOLT-16, SEM, and TANOUE) and colorectal adenocarcinoma cell lines (COLO-320, HCT-15, RKO, SW48, SW480, SW-620, and SW1116). Right, the results of a ChIP experiment where association of the polycomb group protein EZH2, H3K27me3 (repressive mark), and histone H3K4me3 (activating mark) for the aforementioned genes is shown. HOXB13 is included as a positive control of EZH2 binding and H3K27me3 association. DLBCL, diffuse large B-cell lymphomas.

number of targets with a potential role in cancer progression.

Material and Methods

Human cancer cell lines and primary tumor samples

The 102 human cancer cell lines examined were from the American Type Culture Collection and the German Collection of Microorganisms and Cell Cultures (DSMZ). Thirteen tumor types (acute myeloid leukemias, acute lymphoblastic leukemias, lymphomas, colorectal, lung, breast, cervix, ovarian adenocarcinomas, epithelial adenocarcinomas, neuroblastomas, gliomas, osteosarcomas, and teratocarcinomas) were included. DKO, an HCT-116–derived cell line in which 2 major DNA methyltransferases (DNMT1 and DNMT3b) are genetically disrupted, was also used. Cell lines were maintained in appropriate media under confluence. Selected cell lines were treated with 5 μmol/L 5-aza-2′-deoxycytidine (5-aza-dC; Sigma) for 3 or 5 days to achieve demethylation or transfected with *Ikaros* gene to overexpress this protein. A pcDNA3.1-Flag-*Ikaros* construct was generated for ectopic expression of Ikaros. A total of 392 primary tumoral samples corresponding to different tumor types (91 of which were from colorectal adenocarcinoma) and 44 normal samples from different tissues (27 samples were biopsies from normal intestinal tissue) were provided by the CNIO Tumor Bank Unit and the Hematology Service of the Reina Sofia Hospital. All samples were obtained after the donor had given their written informed consent, and the study was approved by the ethical Institutional Review Board.

DNA methylation analysis

DNA methylation analysis was conducted by PCR analysis of bisulfite-modified genomic DNA. Genomic DNA extracted by standard methods was converted by bisulfite modification as described elsewhere (16). The DNA methylation status of all Ikaros family genes was determined by methylation-specific PCR (MSP; ref. 16) and bisulfite genomic sequencing (BS) of a minimum of 10 clones. Primers were designed using the Methyl Primer Express v.1.0 Program (Applied Biosystems; Supplementary Table S1). In primary samples, χ^2 test was used to study the correlation between different clinicopathologic variables and CpG island methylation.

Expression analysis

RNA was isolated by TRIzol extraction (Invitrogen) and reverse transcribed using SuperScript II Reverse Transcriptase (Invitrogen). Primers for conventional and quantitative RT-PCR were designed using Primer3 v.0.4.0 (Supplementary Table S1). Quantitative RT-PCR was carried out in triplicate using 2× SYBR Green PCR Master Mix (Applied Biosystems). PCR reactions were run and analyzed using the Prism 7700 Sequence Detection System (Applied Biosystems). Expression values were normalized against the expression of the endogenous gene controls *RPL38*, *HPRT1*, and *GAPDH*.

For Western blot analyses, nuclear proteins were extracted, purified, and immunoprobed with antibodies against Ikaros (rabbit polyclonal, dilution 1:300; sc-13039; Santa Cruz Biotechnology), Flag M2 (mouse monoclonal, dilution 1:1,000; F1804; Sigma), and Nucleolin (rabbit polyclonal, dilution 1:1,000, sc-13057; Santa Cruz Biotechnology).

Other antibodies used included anti-Meis2 (SAB2101465), anti-Gpx7 (SAB25004872), anti-NHLH1 (SAB2101588), anti-β-actin (A3854; Sigma-Aldrich), anti-GRM2 (19956-1-AP; Protein Tech group), anti-Ptpn6 (610126; BD), and anti-JMJD12 (NB100-77282; Novus Biologicals).

Chromatin immunoprecipitation assay and ChIP-chip analysis

Chromatin was cross-linked by treating cells for 15 minutes with 1% formaldehyde. Then, chromatin was sheared with a Bioruptor (Diagenode) to an average length of 500 bp. Chromatin immunoprecipitation (ChIP) assays were conducted with the aforementioned Ikaros and Flag-M2 antibodies. We also used anti-3meK4H3 (Millipore; 17-614) and anti-3meK27H3 (Millipore; 07-449) to check the presence of these histone modifications at specific sites. Anti-H3 (Abcam; ab 1791) was used as a positive control. In ChIP assays, 5 to 10 μg of each antibody was added to each reaction. Immunoprecipitated chromatin was analyzed by conventional and quantitative PCR. Primers were designed using Primer3 v.0.4.0 (Supplementary Table S1). For the genomic study, immunoprecipitated chromatin was also hybridized in the Human Promoter ChIP-on-chip Microarray Set (Agilent), which analyzes approximately 17,000 of the best-defined human transcripts represented, as defined by RefSeq. Three independent ChIP experiments were carried out for each antibody and the immunoprecipitated material was amplified with a Sigma GenomePlex WGA kit as described (17). Amplified pooled bound and unbound DNA portions were labeled with distinct fluorophores and cohybridized in the microarrays. Genomic segments bound by Ikaros show enrichment of chromatin-immunoprecipitated DNA over the total genomic reference DNA.

Following hybridization, Agilent's Feature Extraction software and ChIP Analytics software were used to quantify images and identify probes corresponding to regions or segments of chromatin that were bound by Ikaros, respectively. Blank subtraction normalization, interarray median normalization, and intra-array (dye-bias) median normalization were applied. Whitehead Error Model v.1.0 and Whitehead Per-Array Neighborhood Model v.1.0 were used with default settings for error modeling and peak detection/evaluation, respectively. Genes common to both anti-Ikaros and anti-Flag-M2 with a greater than 2-fold change were considered to be relevant.

Immunohistochemistry

Two tissue microarray blocks, constructed with duplicate 1-mm diameter cylinders placed on slides coated with 3-aminopropyltriethoxysilane were used. Seventy-four samples were analyzed including 5 normal colon, 7 controls, and 62 biopsies of colon adenocarcinomas. Microwave antigen retrieval and endogenous peroxidase activity and nonspecific binding site blocks were measured. A dilution of 1:10 of antibody against Ikaros as the primary antibody and a dilution of 3:500 of anti-goat as the link were used. Signals were amplified by an indirect Novolink Polymer method (Novocastra) and a 3,3′-diaminobenzidine (DAB) peroxidase developing process coupled with hematoxylin staining was used for detection. Images were acquired using a Leica DM6000B microscope.

Immunofluorescence

Cells were fixed with 4% paraformaldehyde for 30 minutes at room temperature, permeabilized in 0.1% Triton X-100 in PBS for 10 minutes, and stained with the primary antibodies described above. Signals were detected with Alexa Fluor 488–conjugated anti-mouse and anti-rabbit antibodies (Invitrogen) and 4′,6-diamidino-2-phenylindole (DAPI). Fluorescent images were acquired using a Leica SP5 spectral scanning confocal microscope.

Table 1. Methylation analysis of *Ikaros* and *Aiolos* promoter CpG islands in different human leukemia and colorectal adenocarcinoma cell lines and biopsies

Type	Subtype	*n*	Methylation, %	
			Ikaros	*Aiolos*
Leukemia	AML	30	0	3.3
	AML t(8;21)	16	6.2	12.5
	ALL	22	0	0
	CML	14	0	0
Lymphoma	Burkitt	5	15	0
	DLBCL	6	0	0
	Follicular	6	0	0
	Mantle	25	4	0
	Nodal	6	0	0
	Splenic	5	0	0
Normal lymphocyte[a]		5	0	0
Colorectal adenocarcinoma	A Dukes	27	29.6	0
	B Dukes	20	75	0
	C Dukes	22	77.3	0
	D Dukes	22	81.8	0
Normal colon		27	0	0
Normal lung		4	0	0
Breast adenocarcinoma		69	29.9	0
Normal breast		4	0	0
Neuroblastoma		54	27.8	3.7
Glioma		38	50	13.1
Normal brain		4	0	0

NOTE: Colorectal samples are classified into Duke's stages. Fisher's exact test has been used to detect significant differences in methylation between Duke's stages in primary colorectal tumors.

Abbreviations: AML, acute myeloid leukemia; ALL, acute lymphoblastic leukemia; CML, chronic myeloid leukemia.

[a]Used as positive control of nonmethylation.

Colony formation, cell viability, and doubling time assays

For functional assays, pcDNA3.1-Flag-*Ikaros* was transfected by electroporating 10^7 cells with 40 μg of the vector at 250 V and 975 μF. For colony formation assays, different dilutions of transfected cells were plated and cultured at 37°C in a humidified atmosphere of 5% CO_2/95% O_2. After 48 hours of transfection, 500 μg/mL of G418 selection drug was added to the medium. Colonies were fixed and stained with MTT. In cell viability analysis, different dilutions of transfected cells were plated and cultured at 37°C in 5% CO_2/95% O_2 for 5 days. Each day, cells were fixed and stained with MTT and treated with dimethyl sulfoxide. Cell quantities were determined by measuring the optical density at 560 nm. In doubling time assays, the mean time for cell division was measured by counting cells in a Neubauer chamber after treatment with 0.05% trypsin and 0.02% EDTA and trypan blue exclusion. All assays were conducted in triplicate.

Results

Ikaros undergoes distinctive cancer-associated hypermethylation among its homologous family members

To investigate the potential cancer-associated hypermethylation of *Ikaros* family genes, we chose those with bona fide promoter CpG islands, that is, *Ikaros, Helios, Aiolos,* and *Pegasus* (Fig. 1A), whereas Eos, which has a short CpG island around 400 bp downstream of its transcription start site (TSS), was excluded. We conducted DNA methylation screening by MSP and BS in a panel of cell lines that included many tumor types such as hematologic neoplasias, breast, colorectal and lung cancer, neuroblastoma, glioblastoma, and others. The 4 gene promoters were unmethylated in most cell lines (79 of 102) including hematologic cancer cell lines (Fig. 1B and C). These gene promoters were also unmethylated in normal T and B cells, monocytes, and neutrophils (Supplementary Fig. S1). Unexpectedly, the promoter CpG island of Ikaros was densely methylated in all the colorectal cancer cell lines studied (13 of 13; Fig. 1C and Supplementary Fig. S1) but not in normal intestinal tissue (Supplementary Fig. S1).

To determine whether *Ikaros* promoter hypermethylation was also present in primary colorectal tumor samples, we carried out MSP and BS in 91 primary tumor samples, for 27 of which normal matching intestinal samples from the same individuals were available. We observed that around 64% were methylated for *Ikaros*. In contrast, none of the normal 27 paired samples was methylated for *Ikaros*, confirming that *Ikaros* is exclusively methylated in cancer (Table 1 and Supplementary Fig. S1). The proportion of methylated cases increased with advancing Duke's stage (Table 1; 29.6% A; 75.0% B; 77.3% C; and 81.8% D). The χ^2 test confirmed that the increased proportion of hypermethylation between the 3 more

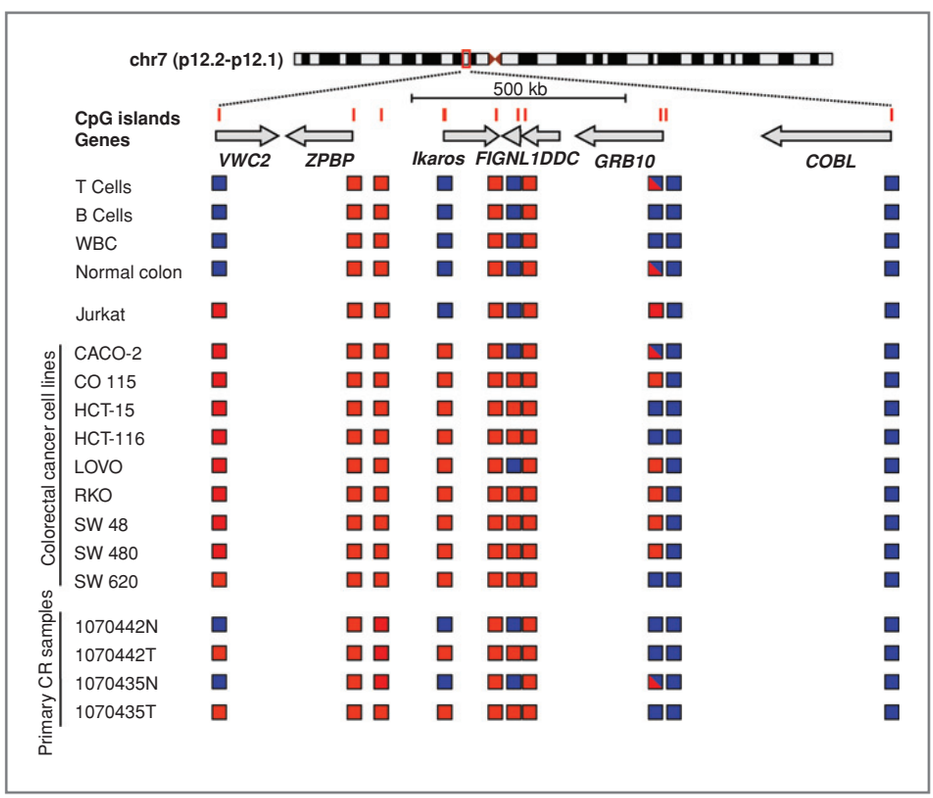

Figure 2. LRES at 7p12.1-7p12.2 is associated with *Ikaros* promoter hypermethylation in colorectal cancer. Diagram depicting the methylation status of the 10 CpG islands spanning ~2 Mb at 7p12.1-7p12.2. The arrows indicate the direction of the genes. Seven of the CpG islands coincide with TSS. Normal T and B cells, white blood cells (WBC), and normal intestinal tissue are shown at the top of the panel. Nine colorectal cancer cell lines and 2 matching pairs of normal intestinal (normal) and colorectal cancer (CR; tumoral) primary samples are included. Red and blue squares respectively indicate hypermethylation and hypomethylation, respectively.

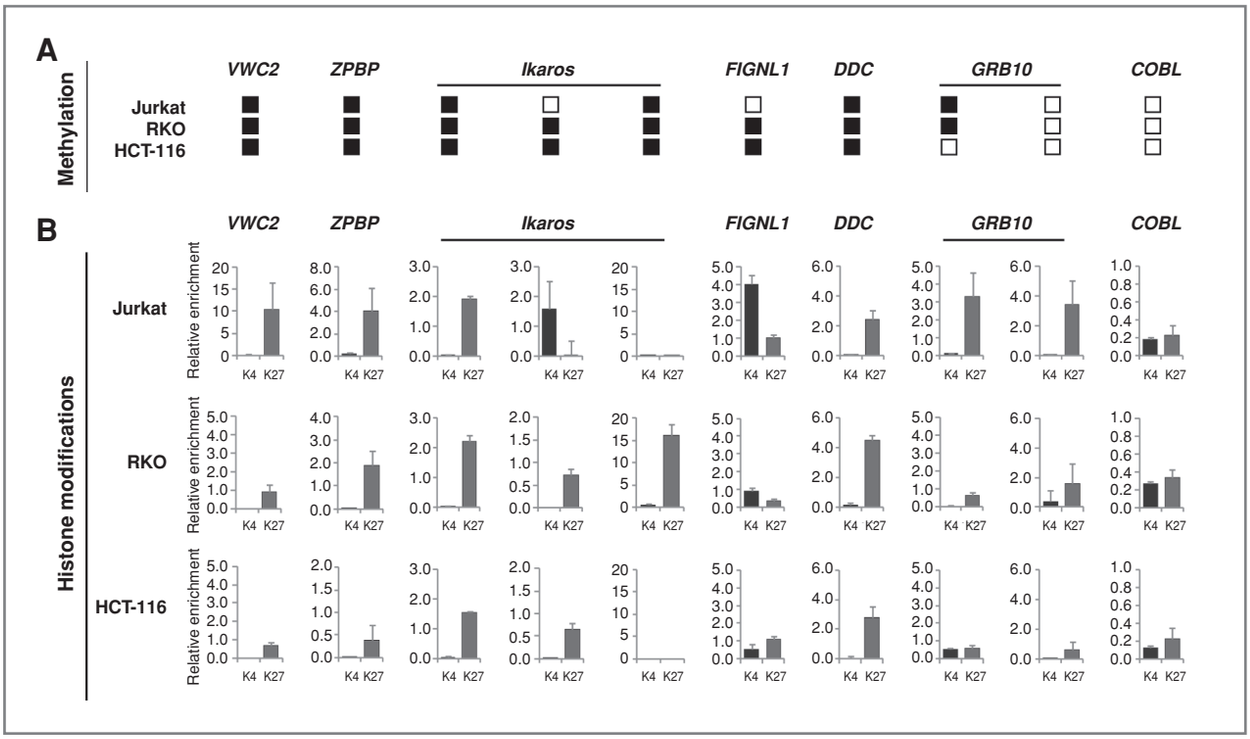

Figure 3. Epigenetic landscape of the CpG islands located within the 7p12.1-7p12.2 region. A, methylation status of the 10 CpG islands in Jurkat T leukemia cells and the colorectal cancer cell lines RKO and HCT-116. Empty and filled squares respectively indicate unmethylated and methylated status. B, ChIP analysis showing the levels of H3K4me3 (noted as K4) and H3K27me3 (noted as K27) for the 10 CpG islands in Jurkat, RKO, and HCT-116 cells.

advanced Duke's stages (B–D) and A Duke's stage samples was significant ($P = 0.0035$; $P = 0.0039$; $P = 0.0005$), indicating that *Ikaros* hypermethylation could be used as a marker of colorectal cancer progression. No significant correlations were found between hypermethylation and age ($P = 0.792$), gender ($P = 0.094$), or tumor localization ($P = 0.643$) as concluded after using χ^2 test.

Ikaros's very specific promoter hypermethylation in colorectal cancer cell lines and primary colorectal tumors was particularly striking when compared with the absence of DNA methylation found for all other *Ikaros* family members, with whom *Ikaros* shares abundant similarities at the regulatory level. For instance, Ikaros, Helios, and Aiolos had similar expression levels for lymphoid neoplasias (highly expressed) and colorectal cancer cell lines (low expression levels; Fig. 1D, left). We wondered whether different methylation status of *Ikaros* in colorectal cancer cells was associated with a distinctive histone modification profile at its promoter. Specifically, we compared the presence at the *Ikaros*, *Helios*, and *Aiolos* promoters of histone H3 K4 trimethylation (H3K4me3), associated with active transcription, trimethylation of K27 H3 (H3K27me3), that correlates with repression, and association of the member of the polycomb group family EZH2, which often correlates with CpG island hypermethylation (5, 6) and targets H3K27me3. The activating mark H3K4me3 was present in Jurkat T cells for all 3 gene promoters, consistent with transcription of these genes in T cells, whereas it was absent from HCT-116 colorectal cancer cells (Fig. 1D, right). EZH2 and H3K27me3 were absent at the *Ikaros* and *Helios* gene promoters in both Jurkat and HCT-116 cells. The only gene that had EZH2 and H3K27me3 associated with its promoter in colorectal cancer cells was *Aiolos*, which does not undergo hypermethylation (Fig. 1D, right). In conclusion, specific hypermethylation of *Ikaros* in colorectal cancer cells did not correlate with EZH2 association at its promoter.

Ikaros is located in an LRES region and undergoes methylation in colorectal cancer

As mentioned above, recent genome-scale analyses have identified large chromosomal regions containing several CpG island often hypermethylated and transcriptionally repressed termed as LRES (7–11, 18). LRES is frequent in colorectal cancer (7, 11). Given the absence of EZH2 targeting to the *Ikaros* promoter, we wondered whether its hypermethylation in colorectal cancer is associated with an LRES event. To address this possibility, we analyzed all the CpG islands within a 2-Mb region centered on *Ikaros* in normal T and B cells and in normal intestinal cells. This region located on chromosome 7p12.1-7p12.2 contains 10 CpG islands, including the *VWC2*, *ZPBP*, *Ikaros*, *FIGNL1*, and *COBL* promoters, 2 intergenic regions, and the 2 CpG

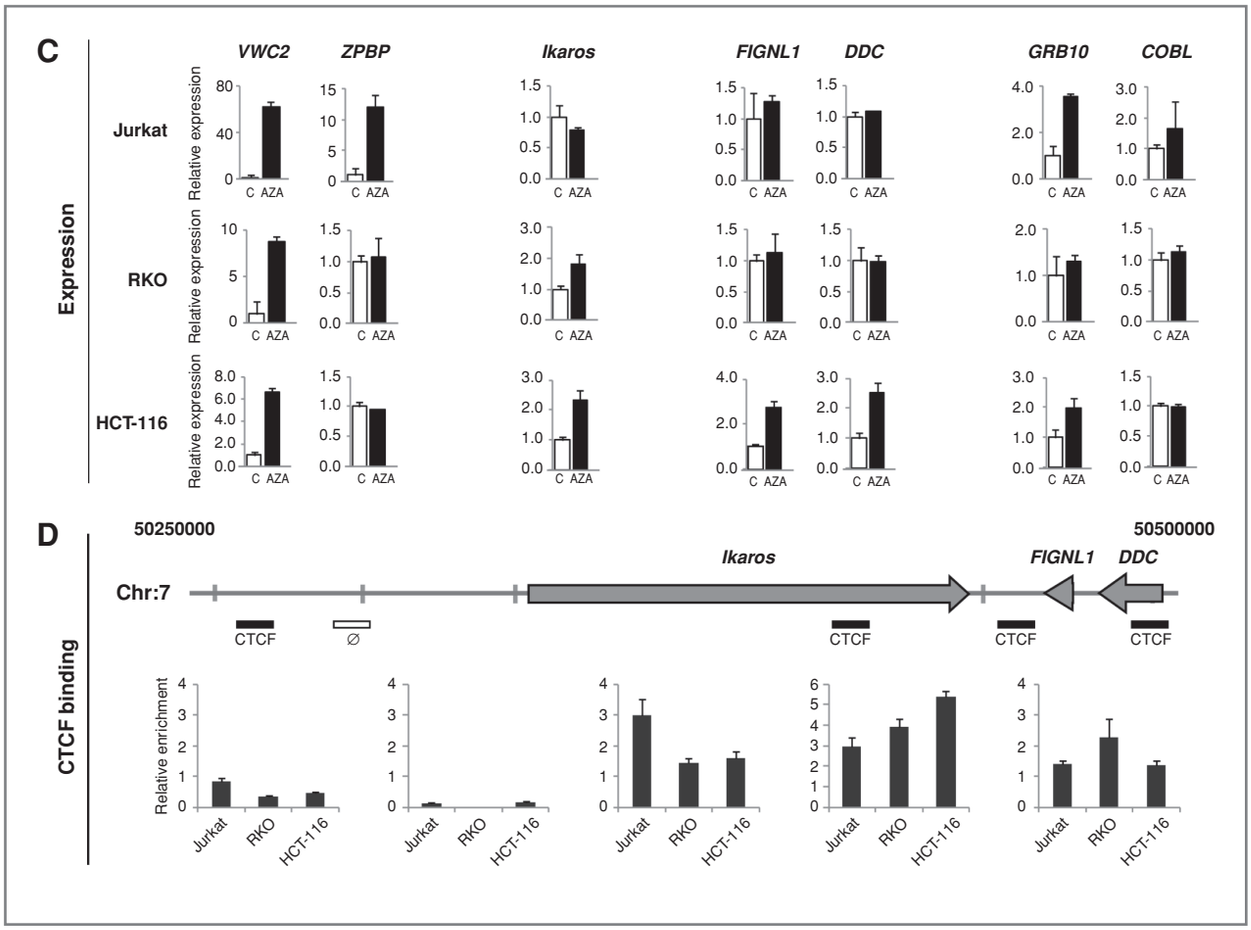

Figure 3. (*Continued*) C, expression data for the 7 genes within the 7p12.1-7p12.2 region in the 3 cell lines before and after treatment with the demethylating agent 5-aza-dC. Data relative to the expression of RPLR38. D, scheme depicting the region centered in Ikaros where 4 CTCF-binding sites (from reference 21; accession number SRA000206) are indicated with black bars. An additional sequence in the region was as a negative control (indicated with an empty bar). ChIP data with anti-CTCF antibodies are presented for Jurkat, RKO, and HCT-116 cells.

islands associated with 2 alternative TSS of the imprinted gene *GRB10* (19). Our results showed that this 2-Mb region exhibits a complex pattern of CpG island methylation where 4 of the 10 CpG islands are methylated in normal cells (Fig. 2). In all colorectal cancer cell lines, we observed that at least 3 additional CpG islands in the region, including *Ikaros*, *VWC2*, and *FIGNL1* promoters, are hypermethylated (Fig. 2). We also determined the methylation status of these CpG islands for the glioma (U-87 MG) and breast cancer (MDA-MB-231) cell lines for which *Ikaros* is hypermethylated (Fig. 1D). Again, we observed that those cell lines had 7 of the 10 CpG islands at 7p12.1-7p12.2 hypermethylated (not shown). We observed an identical pattern of CpG island methylation in primary colorectal adenocarcinoma samples (Fig. 2 and Supplementary Fig. S2A). Remarkably, when analyzing the potential relationships between the DNA methylation status of VWC2 and FIGNL1 and Duke's stage, the results obtained were not statistically significant ($P = 0.753$; $P = 0.820$; Supplementary Fig. S2B and C), in contrast with those obtained for *Ikaros*, suggesting that the spread of methylation in the region during cancer progression varies from gene to gene within the LRES band.

To address whether the hypermethylated status of these CpG islands at 7p12.1-7p12.2 was associated with a specific profile of histone modifications, we analyzed the presence of H3K4me3 and H3K27me3 in Jurkat T cells, where *Ikaros* and *FIGNL* are nonmethylated (Fig. 3A), and the colorectal cancer cell lines HCT-116 and RKO, where 8 of the 10 CpG islands are hypermethylated including *Ikaros, VWC2*, and *FIGNL* (Fig. 3A). In general, the entire region exhibited enrichment in the repressive mark H3K27me3, and very low levels of the active mark H3K4me3 were observed (Fig. 3B). Interestingly, *Ikaros* and *FIGNL* had H3K4me3 associated to their promoters in Jurkat T cells, where these 2 genes are nonmethylated. In contrast, these 2 genes had lower levels or absence of this mark in HCT-116 and RKO cells, where they are hypermethylated. We treated these 3 cell lines with the demethylating agent 5-aza-dC and observed that induced demethylation of these genes resulted in reactivation of most genes, except those situation where the genes were already demethylated like *Ikaros* or *FIGNL1*

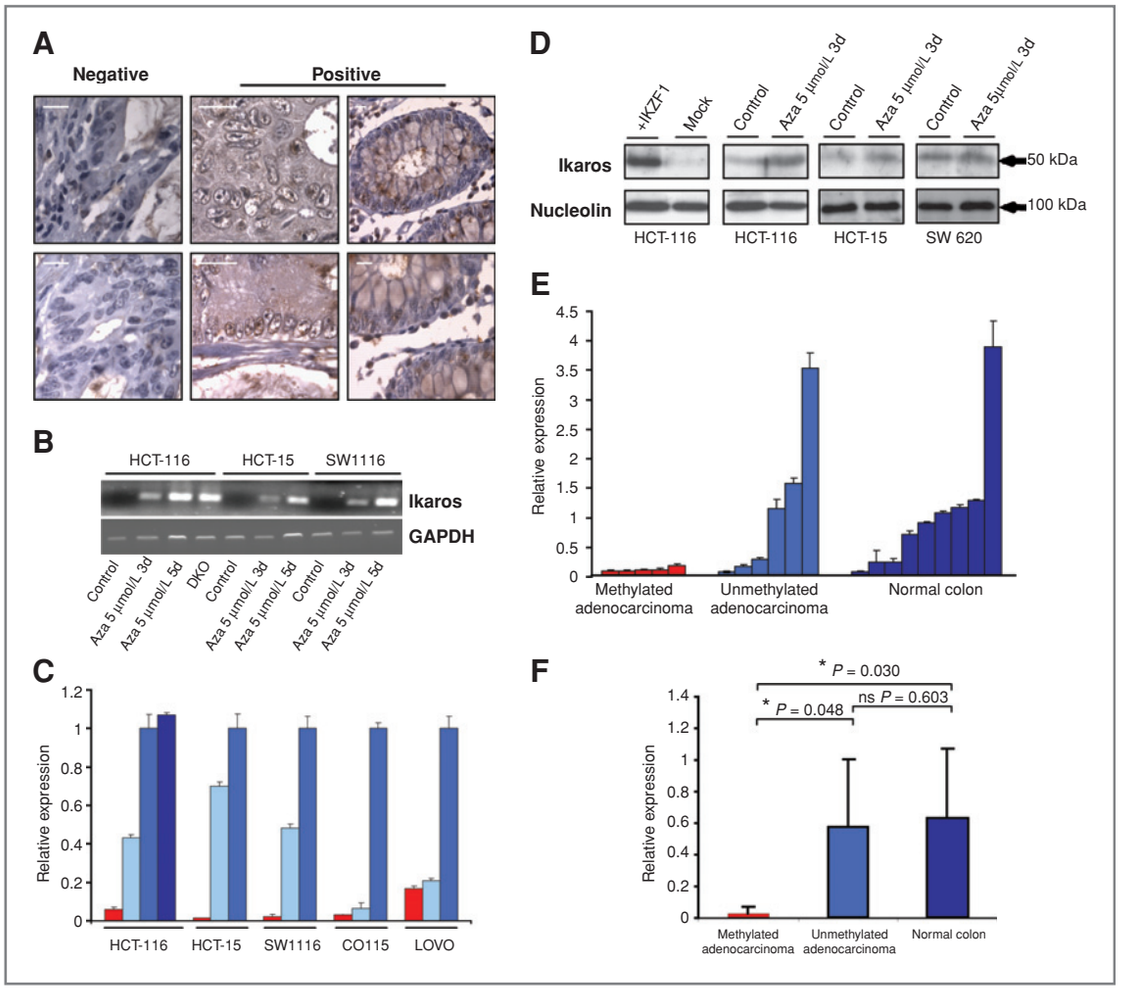

Figure 4. Abrogation of expression of Ikaros in colorectal cancer is methylation dependent. A, immunohistochemistry of Ikaros in human primary colorectal cancer tumors. Examples of both negative and positive expression are shown. B, RT-PCR analysis of Ikaros reexpression following 5-aza-dC (3 and 5 days) treatment in 3 different colorectal cancer cell lines. HCT-116 double knockout cells for DNMT1a and DNMT3b are also included. GAPDH is used as a control. C, quantitative real-time analysis of Ikaros expression following 5-aza-dC treatment. Control cells are represented with red bars, cells treated without 5 μmol/L aza-dC are represented with 2 different blue tones, and DKO cells (HCT-116 cells deficient for DNMT3a and DNMT3b) are also included and represented with dark blue. D, Western blot analysis showing the effects of 5-aza-dC on expression levels of Ikaros in HCT-116 cells. E, relative expression analyzed by quantitative real-time PCR of Ikaros in primary colorectal adenocarcinoma samples and controls. Samples have been grouped according to the methylation status of *Ikaros* promoter CpG island. F, average relative expression values for different groups of primary colorectal samples (normal, unmethylated, and methylated for Ikaros) analyzed by quantitative real-time PCR. GAPDH, glyceraldehyde-3-phosphate dehydrogenase; ns, nonsignificant.

in Jurkat cells (Fig. 3C). We wondered whether the observed methylation changes within the region could also associate with changes in the binding of the enhancer-blocking transcription factor CTCF, which is known to bind DNA in a methylation-specific manner (20). For that, we analyzed 4 described CTCF-binding sites in the vicinity of *Ikaros* (accession number: SRA000206; ref. 21). We also included an additional short sequence in the same region as a negative control for CTCF binding. ChIP analysis of the 4 binding sites revealed reduced association of CTCF to the binding site located in the *Ikaros* coding region when comparing the 2 colorectal cancer cell lines with Jurkat cells (Fig. 3D).

Complete loss of expression of *Ikaros* in colorectal cancer is dependent on DNA methylation

Ikaros is primarily expressed at different stages of the lymphoid branch. By using immunostaining, we investigated the levels of Ikaros in primary colorectal tissues and adenocarcinoma samples. Immunohistochemistry revealed the existence of a subset of primary colorectal adenocarcinoma samples and normal colon with positive nuclear staining for Ikaros (Fig. 4A). We also investigated the dependence on DNA methylation for the expression status of *Ikaros* in the context of intestinal colorectal tissue. We first analyzed the levels of Ikaros mRNA in several colorectal cancer cell lines by quantitative real-time PCR and

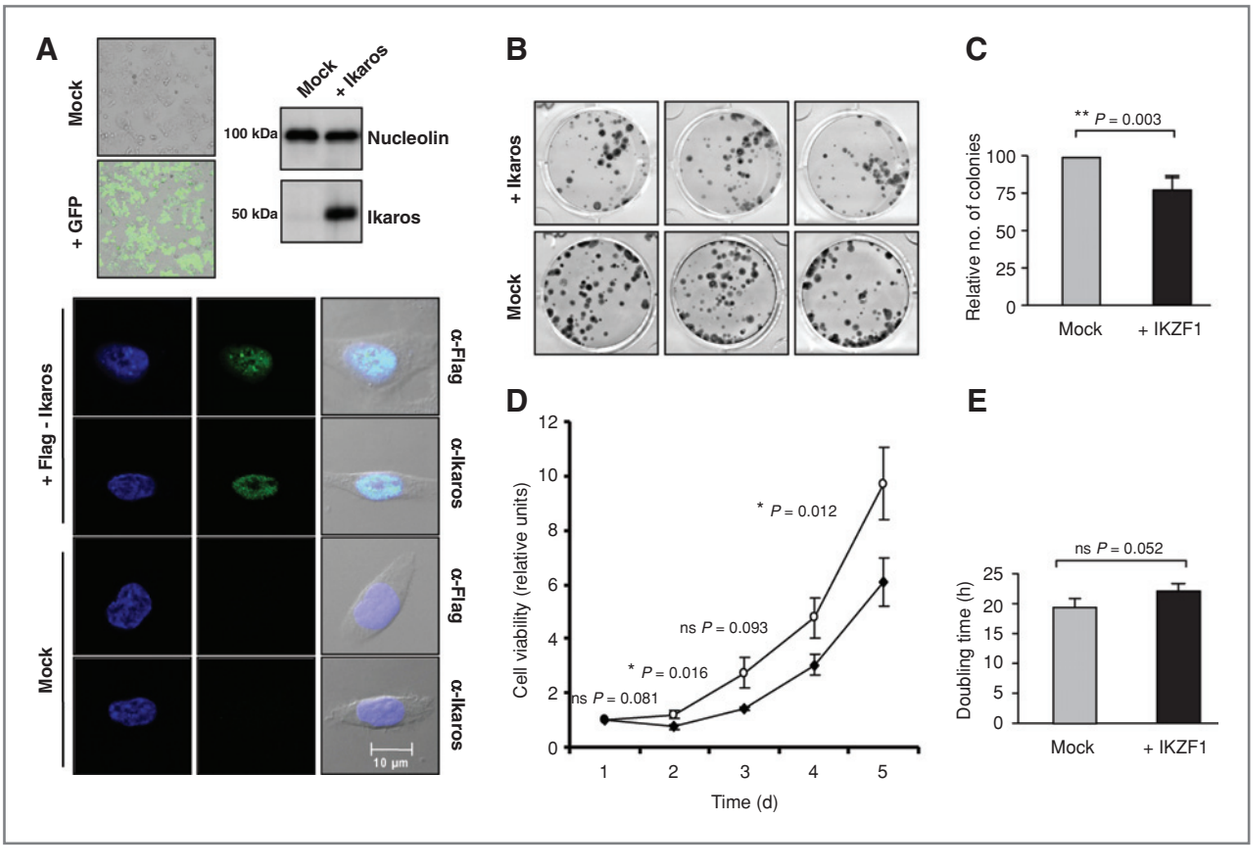

Figure 5. Functional effects of Ikaros ectopic expression in HCT-116 cells. A, ectopic expression of Ikaros in HCT-116 cells. Top left, efficiency of transfection was estimated to be around 80% by using parallel transfection with a GFP-tagged vector. Top right, expression of Ikaros in HCT-116 cells following transfection as shown by Western blotting. Bottom, cellular localization of Ikaros. Confocal images of HCT-116 cells transfected with Ikaros expression vector or empty vector and labeled with antibodies to Ikaros and M2-FLAG (green). DNA was counterstained with DAPI (blue). B, effect of Ikaros transfection on *in vitro* colony formation properties of transfected HCT-116 cancer colon cells. Mock-transfected cells are shown in parallel. Examples (in triplicate) of colony formation assay after a 2-week selection of G418 stained with MTT reagent. C, percentage of colony numbers normalized with focus number of HCT-116 transfected with the empty vector. The HCT-116 mock was set at 100%. Results are an average of triplicates of 3 independent experiments. D, cell viability determined by MTT assay monitoring the number of cells over time after transfecting HCT-116 with Ikaros and the empty vector. E, doubling time of HCT-116 cells transfected with Ikaros and empty vector. Cells were stained with trypan blue and counted over time. Doubling time = time between 2 measurements × ln2/ln(final concentration/initial concentration). The outcome was measured as the average of triplicates of 3 independent experiments and its SD. GFP, green fluorescent protein.

monitored the consequences of treatment with the demethylating agent 5-aza-dC. This treatment resulted in partial demethylation (Supplementary Fig. S1) and the expression of *Ikaros*. This increase in expression was observed at the mRNA and protein levels, suggesting that expression of Ikaros in these colorectal cancer cell lines is DNA methylation dependent (Fig. 4B–D).

We then compared the transcript levels of *Ikaros* in normal colon, in which *Ikaros* is unmethylated, and 2 sets of primary colorectal cancer samples for which we had previously determined the DNA methylation status of the *Ikaros* promoter CpG island (Table 1). Despite the broad range of *Ikaros* mRNA levels, we found similar levels of expression of *Ikaros* between primary tumors samples unmethylated for *Ikaros* and normal colon, whereas *Ikaros*-hypermethylated primary samples exhibited absence of expression (Fig. 4E and F).

Ectopic expression of Ikaros in HCT-116 cells

We next explored the functional implications of *Ikaros* epigenetic silencing in colorectal cells. To this end, we ectopically expressed the full-length isoform of Ikaros in HCT-116 cells. In these experiments, we typically found around 80% of transfection efficiency and confirmed that transfection of Ikaros in colorectal cells was accompanied by expression of the protein and proper nuclear distribution (Fig. 5A).

We then examined whether the presence or absence of Ikaros affected growth. Colony formation assays showed that reintroduction of Ikaros in HCT-116 significantly reduced colony formation (by around 25%; Fig. 5B and C). Cell viability assays were also conducted to compare Ikaros-transfected HCT-116 cells with empty vector–transfected cells. Introduction of Ikaros produced a significant reduction in cell viability (by 25%–30%) as determined by

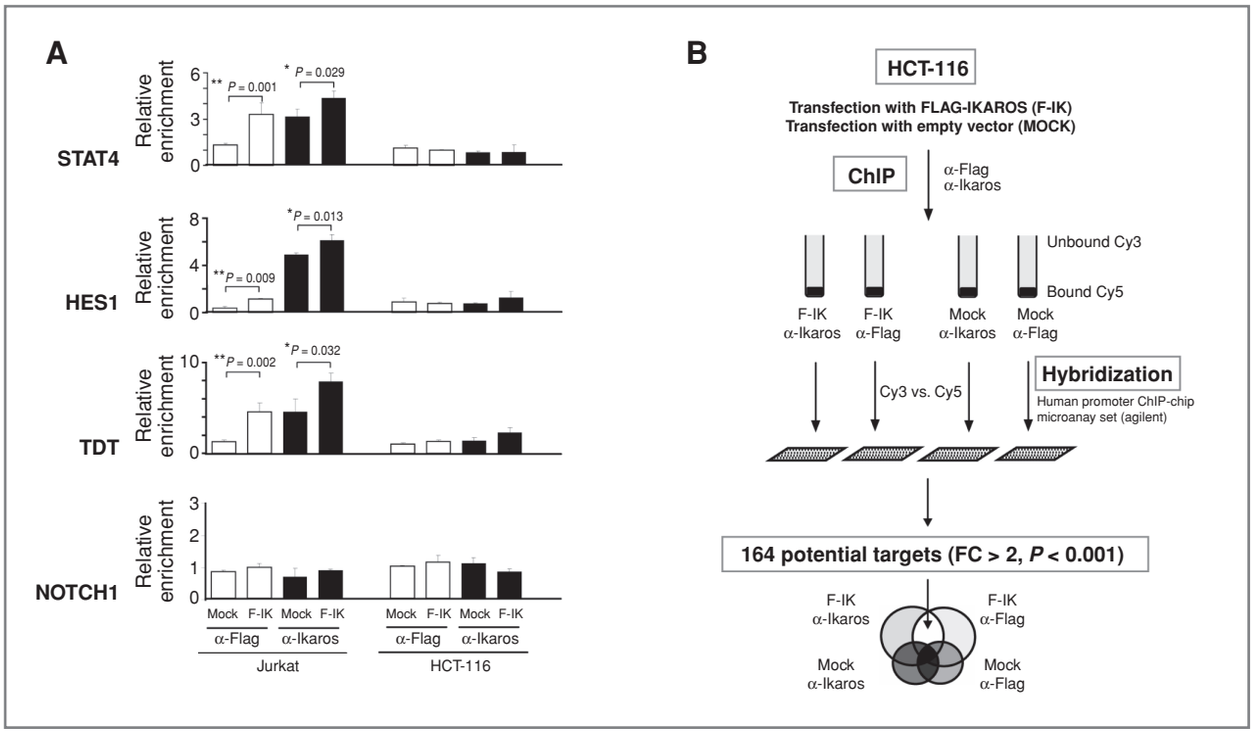

Figure 6. Analysis of Ikaros targets. A, quantitative ChIP analysis of known Ikaros targets in human hematologic (Jurkat cell line) and colorectal (HCT-116 cell line) contexts. Cell lines transfected with Flag-Ikaros expression vector (F-IK) or empty vector (mock) were immunoprecipitated with antibodies against Ikaros or M2-Flag. *P* values are shown for each comparison (values of $P < 0.05$ were taken to be statistically significant). B, diagram depicting the rationale of the ChIP-chip experiment. The 164 potential targets result from overlapping the results obtained from the 2 different antibodies in Flag-Ikaros–transfected cells and subtracting the values obtained from mock-transfected cells.

MTT assay (Fig. 5D). Finally, the doubling time of Ikaros transfected was around 10% longer than in empty vector–transfected cells (Fig. 5E).

Identification of Ikaros direct targets in colorectal cells

Given that Ikaros is a transcription factor, we sought to identify targets in the context of colorectal cells. Until now, there are no high-throughput analysis on Ikaros targets, although several studies have identified some in T lymphoid cells (22–24). To determine whether these bona fide Ikaros targets were also directly regulated in the context of colorectal cancer cells, we conducted ChIP assays in both Ikaros-transfected HCT-116 cells and Jurkat T-cell leukemia cells, a well-studied T-cell leukemia cell line, as a positive control. Two antibodies, anti-Ikaros and anti-FLAG, were used. We then amplified the immunoprecipitated material with primers complementary to the promoter of 3 direct targets for Ikaros in T cells, specifically TDT, STAT4, and the Notch target gene *HES-1* (22–24), and an additional gene of the Notch pathway, *NOTCH1*, which has not been described as being a direct target of Ikaros. ChIP experiments showed that Ikaros binds to the proximal promoter of TDT, HES-1, and STAT4 in Jurkat T cells but not in HCT-116 cells (Fig. 6A). This result suggests that the identity of Ikaros targets depends on the cell type and is probably determined by specific chromatin scenarios.

To identify Ikaros targets in the context of HCT-116 cells, we conducted ChIP assays and hybridized the immunoprecipitated material in proximal promoter microarrays (Fig. 6B). ChIP assays were conducted in Ikaros- and mock-transfected HCT-116 cells with both anti-Ikaros and anti-FLAG antibodies. We compared the anti-Ikaros and anti-FLAG binding sites in Ikaros-transfected HCT-116 samples with respect to mock-transfected samples to exclude nonspecific signal. In total, we identified 164 Ikaros-bound chromatin segments. Genes common to anti-Ikaros and anti-Flag with a greater than 2-fold change were considered to be relevant (Supplementary Table S2 and see also Fig. 6B). A significant overlap between the anti-Ikaros and anti-FLAG profiles of association was observed. Among the genes identified, we found several genes for which an association with colorectal adenocarcinoma had previously been reported, such as *PTPN6* (25), which codes for protein tyrosine phosphatase, nonreceptor type; *MEIS2* (26), a homeobox protein coding gene; and *GPX7* (27), the glutathione peroxidase 7 gene.

We then sought to confirm the binding of Ikaros to the promoter of a selection of 25 significant genes resulting from the ChIP-chip experiment on the basis of those that were most highly enriched, or that might be relevant to cancer progression (highlighted in blue in Supplementary Table S2). We analyzed expression by quantitative real-time

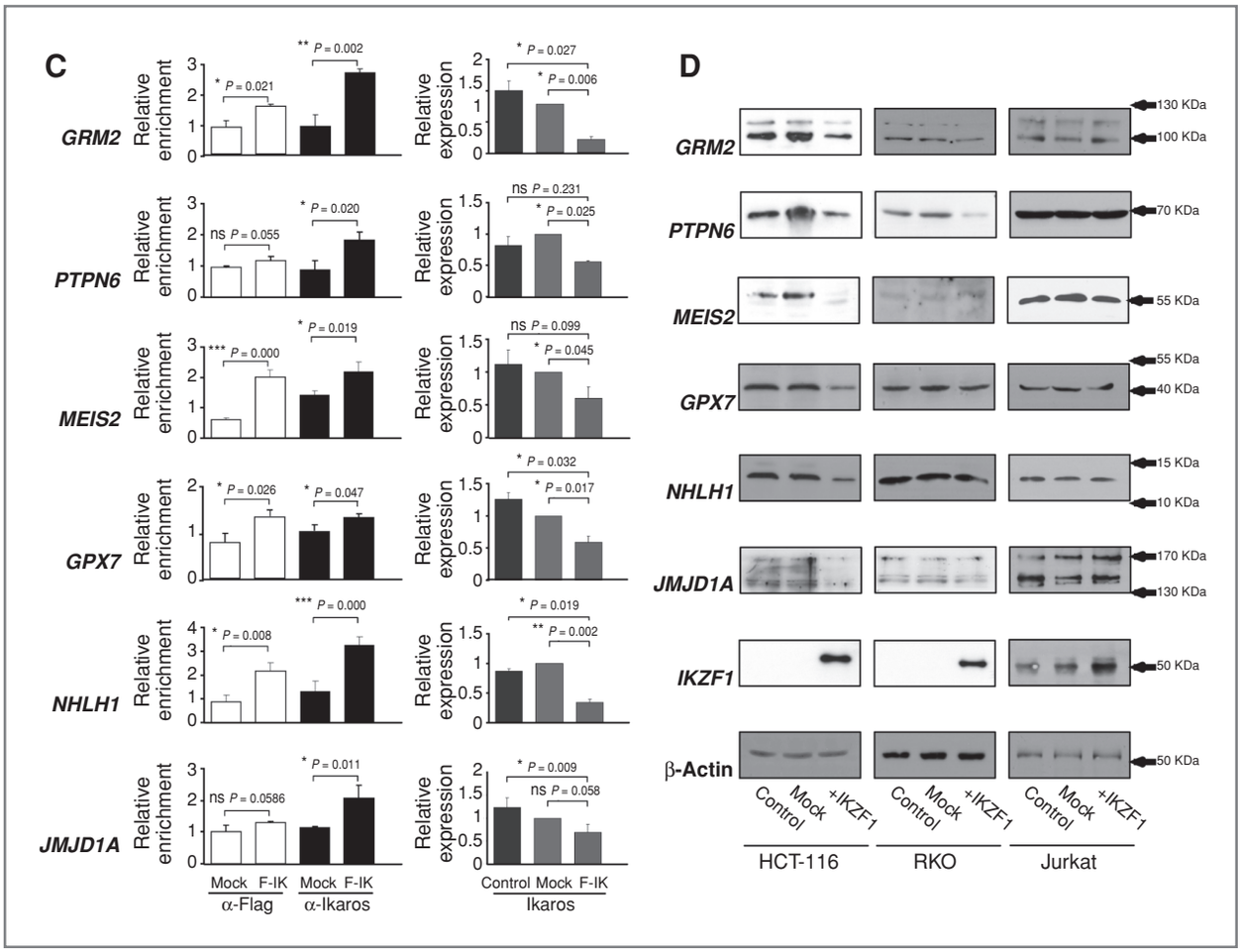

Figure 6. (*Continued*) C, quantitative ChIP and quantitative RT-PCR analysis of several Ikaros targets. HCT-116 cells were transfected with Ikaros expression vector (F-IK) or empty vector (mock) and immunoprecipitated with antibodies against Ikaros or M2-Flag. *P* values are shown for each comparison (values of $P < 0.05$ were taken to be statistically significant). D, Western blot analysis of several Ikaros targets in HCT-116 and RKO (colorectal) an Jurkat cells (T-cell leukemia) following transfection with Ikaros.

RT-PCR to identify the direct effects on these Ikaros targets and found that 10 of the 25 selected genes were more weakly expressed following Ikaros reintroduction in HCT-116 cells, showing that these genes are directly downregulated by Ikaros (Fig. 6C, right). Among the genes whose expression levels significantly changed were *PTPN6*, *GRM2*, *MEIS2*, *GPX7*, *NHLH1*, *HNRPD1*, *JMJD1A*, *RAB23*, *BCL-X*, *RFT-1*, and *TRPV2*. This decrease is consistent with the repressive role of Ikaros (28). Individual ChIP analysis confirmed the binding of Ikaros to the promoter region of the genes validated above (Fig. 6C, left). The effects on expression were also analyzed at the protein level in the 2 colorectal cancer cell lines HCT-116 and RKO, as well as in Jurkat T cells. Several of these targets, such as GRM2, PTPN6, or MEIS2, showed a decrease in their levels in HCT-116 and RKO cells following reintroduction of Ikaros (Fig. 6D). Altogether, these results indicate that direct binding of Ikaros in the promoter of these genes contributes to their downregulation in normal colorectal tissue and that aberrant epigenetic inactivation of Ikaros is directly associated with their overexpression.

Ikaros direct targets are deregulated in primary colorectal tumor samples

Our next step was to confirm whether Ikaros targets validated in the context of HCT-116 cells were also deregulated in primary colorectal tumor samples. We carried out quantitative real-time PCR for all primary tumors and found significant differences in the expression levels with respect to the methylation status of Ikaros promoter CpG island in several of the aforementioned genes, including *PTPN6*, *GRM2*, *MEIS2*, and *GPX7* (Supplementary Fig. S3). This result reinforces the notion that *Ikaros* epigenetic inactivation may directly affect the upregulation of these targets in the context of colorectal cancer.

Discussion

Our results provide evidence that an LRES event is associated with hypermethylation of the *Ikaros* promoter CpG island and that *Ikaros* epigenetic silencing results in the deregulation of several of its targets in the context of colorectal adenocarcinoma.

Our initial DNA methylation screening showed that *Ikaros* promoter, in contrast with the rest of the *Ikaros* gene family, is heavily methylated in colorectal cancer cells. We first investigated the potential association of a specific histone modification profile and binding of polycomb group member EZH2 with the promoter of *Ikaros*, as well as all the other members of its family, given the reported relationship between these marks and aberrant hypermethylation in cancer (5, 6). However, no association of EZH2 or H3K27me3 was found at the *Ikaros* promoter in colorectal cancer cells. We also investigated whether changes in the DNA methylation status of the neighboring regions of *Ikaros* could explain its distinct behavior from that seen in the rest of the family. We found that *Ikaros* is embedded in an LRES region. Our findings suggest that chromosomal context of *Ikaros* is responsible for its distinctive hypermethylation in colorectal adenocarcinoma. This could explain why *Ikaros* behaves differently from the other family members, with which *Ikaros* shares regulatory elements.

The mechanism involved in LRES is under debate. It has been proposed that if some CpG island genes are targeted for methylation, neighboring genes may also be affected by default (10). Perhaps, LRES might be initiated by 1 critical gene target that spreads and conscripts "innocent bystanders," analogous to large genetic deletions (18). In the case of the 7p12.1-12.2 region, we have observed that 4 of the 10 CpG islands in the region are already methylated in normal cells. We can speculate whether *GRB10*, a well-studied imprinted gene (19), is associated with the spread of hypermethylation across this chromosomal region. In all colorectal cancer cell lines and primary adenocarcinomas, as well as in 2 additional breast cancer and glioma cell lines, we have observed hypermethylation of 3 additional CpG islands within the region.

Our study reveals that hypermethylation of *Ikaros* occurs in a tumor-specific manner and appears to be associated with more aggressive forms according to the proportion of *Ikaros* methylation in relation to the Duke's stage, which occur in a coordinated manner with the neighboring genes *VWC2* and *FIGNL*.

To the best of our knowledge, our study is the first report of genetic or epigenetic changes of an *Ikaros* family member outside of a hematologic malignancy, where *Ikaros* is expressed at very low levels. We were able to detect low but reproducible levels of expression of Ikaros in normal colon and unmethylated colorectal adenocarcinoma samples. Although reintroduction of Ikaros in HCT-116 moderately affects cell viability and growth, these experiments allowed us to identify a number of direct Ikaros targets, some of which are also deregulated in primary cases. The importance of the genes identified by ChIP-chip analysis as targets of Ikaros in the context of colorectal cancer becomes more evident when gene ontology analysis is carried out and in the light of existing published studies. Among the genes shown to feature binding to Ikaros, we found several notable markers, some of which had been previously referenced in the context of colorectal cancer. For instance, *PTPN6*, which, like Ikaros, is primarily expressed in hematopoietic cells, has been proposed to play either a negative or a positive role in regulating signal transduction pathways in lymphoma, leukemia, and other cancers, as it functions as an antagonist to the growth-promoting and oncogenic potentials of tyrosine kinase. Interestingly, PTPN6 is normally expressed or overexpressed in some nonlymphocytic cell lines such as prostate, ovarian, and breast cancer cell lines. The level of PTPN6 expression is also altered in some breast cancer cell lines with negative expression of estrogen receptor, and in some prostate and colorectal cancer cell lines (25). MEIS2 belongs to a group of homeobox cofactors for HOX-class homeobox proteins, which control growth and differentiation during embryogenesis and homeostasis, and has been implicated in various cancer types. Deregulation of *GPX7* (27), a glutathione peroxidase, or *GRM2*, gene related to metastasis 2, have also been with cancers including colorectal adenocarcinoma. Finally, NHLH1 belongs to a helix-loop-helix family of putative transcription factors that have been implicated in tumorigenesis.

Our investigation highlights how the chromosomal neighborhood, and perhaps a tissue-specific chromatin context, could influence the permissivity to become hypermethylated. In this case, this effect appears to be more relevant than other factors shared by the rest of the *Ikaros* family members. Although the occurrence of these hypermethylation changes might not necessarily be associated with functional changes, in the case of Ikaros, we find that its hypermethylation-associated erasure of expression in colorectal cancer appears to have functional consequences in the aberrant expression of a number of targets.

Disclosure of Potential Conflicts of Interest

No potential conflicts of interest were disclosed.

Acknowledgment

The authors thank Drs. Miguel Angel Peinado, Dave Monk, and Maribel Parra for their helpful comments and the Spanish National Tumor Bank Network, especially Dr. Maria Jesus Artiga, for providing us with primary samples.

Grant Support

E. Ballestar is supported by PI081346 grant from the Spanish Ministry of Science and Innovation (MICINN-ISCIII) and 2009SGR184 AGAUR grant (Catalan Government). B.M. Javierre is funded by a BEFI Predoctoral Fellowship from ISCIII, Spain.

The costs of publication of this article were defrayed in part by the payment of page charges. This article must therefore be hereby marked *advertisement* in accordance with 18 U.S.C. Section 1734 solely to indicate this fact.

Received November 15, 2010; revised June 21, 2011; accepted June 28, 2011; published OnlineFirst July 7, 2011.

References

1. Jones PA, Baylin SB. The epigenomics of cancer. Cell 2007;128: 683–92.
2. Costello JF, Frühwald MC, Smiraglia DJ, Rush LJ, Robertson GP, Gao X, et al. Aberrant CpG-island methylation has non-random and tumour-type-specific patterns. Nat Genet 2000;24:132–8.
3. Esteller M, Corn PG, Baylin SB, Herman JG. A gene hypermethylation profile of human cancer. Cancer Res 2001;61:3225–9.
4. Keshet I, Schlesinger Y, Farkash S, Rand E, Hecht M, Segal E, et al. Evidence for an instructive mechanism of *de novo* methylation in cancer cells. Nat Genet 2006;38:149–53.
5. Schlesinger Y, Straussman R, Keshet I, Farkash S, Hecht M, Zimmerman J, et al. Polycomb-mediated methylation on Lys27 of histone H3 pre-marks genes for *de novo* methylation in cancer. Nat Genet 2007;39:232–6.
6. Widschwendter M, Fiegl H, Egle D, Mueller-Holzner E, Spizzo G, Marth C, et al. Epigenetic stem cell signature in cancer. Nat Genet 2007;39:157–8.
7. Frigola J, Song J, Stirzaker C, Hinshelwood RA, Peinado MA, Clark SJ, et al. Epigenetic remodeling in colorectal cancer results in coordinate gene suppression across an entire chromosome band. Nat Genet 2006;38:540–9.
8. Dallosso AR, Hancock AL, Szemes M, Moorwood K, Chilukamarri L, Tsai HH, et al. Frequent long-range epigenetic silencing of protocadherin gene clusters on chromosome 5q31 in Wilms' tumor. PLoS Genet 2009;5:e1000745.
9. Hsu PY, Hsu HK, Singer GA, Yan PS, Rodriguez BA, Liu JC, et al. Estrogen-mediated epigenetic repression of large chromosomal regions through DNA looping. Genome Res 2010;20:733–44.
10. Coolen MW, Stirzaker C, Song JZ, Statham AL, Kassir Z, Moreno CS, et al. Consolidation of the cancer genome into domains of repressive chromatin by long-range epigenetic silencing (LRES) reduces transcriptional plasticity. Nat Cell Biol 2010;12:235–46.
11. Mayor R, Casadomé L, Azuara D, Moreno V, Clark SJ, Capellà G, et al. Long-range epigenetic silencing at 2q14.2 affects most human colorectal cancers and may have application as a non-invasive biomarker of disease. Br J Cancer 2009;100:1534–9.
12. Cortes M, Wong E, Koipally J, Georgopoulos K. Control of lymphocyte development by the Ikaros gene family. Curr Opin Immunol 1999;11:167–71.
13. Mullighan CG, Goorha S, Radtke I, Miller CB, Coustan-Smith E, Dalton JD, et al. Genome-wide analysis of genetic alterations in acute lymphoblastic leukaemia. Nature 2007;446:758–64.
14. Mullighan CG, Miller CB, Radtke I, Phillips LA, Dalton J, Ma J, et al. BCR-ABL1 lymphoblastic leukaemia is characterized by the deletion of Ikaros. Nature 2008;453:110–4.
15. Mullighan CG, Su X, Zhang J, Radtke I, Phillips LA, Miller CB, et al. Deletion of Ikaros and prognosis in acute lymphoblastic leukemia. N Engl J Med 2009;360:470–80.
16. Herman JG, Graff JR, Myöhänen S, Nelkin BD, Baylin SB. Methylation-specific PCR: a novel PCR assay for methylation status of CpG islands. Proc Natl Acad Sci U S A 1996;93:9821–6.
17. O'Geen H, Nicolet CM, Blahnik K, Green R, Farnham PJ. Comparison of sample preparation methods for ChIP-chip assays. Biotechniques 2006;41:577–80.
18. Clark S. Action at a distance: epigenetic silencing of large chromosomal regions in carcinogenesis. Hum Mol Genet 2007;16: R88–95.
19. Monk D, Arnaud P, Frost J, Hills FA, Stanier P, Feil R, et al. Reciprocal imprinting of human GRB10 in placental trophoblast and brain: evolutionary conservation of reversed allelic expression. Hum Mol Genet 2009;18:3066–74.
20. Bell AC, Fesenfeld G. Methylation of a CTCF-dependent boundary controls imprinted region of the Igf2 gene. Nature 2000;405: 482–5.
21. Barski A, Cuddapah S, Cui K, Roh TY, Schones DE, Wang Z, et al. High-resolution profiling of histone methylations in the human genome. Cell 2007;129:823–37.
22. Kathrein KL, Chari S, Winandy S. Ikaros directly represses the notch target gene Hes1 in a leukemia T cell line: implications for CD4 regulation. J Biol Chem 2008;283:10476–84.
23. Yap WH, Yeoh E, Tay A, Brenner S, Venkatesh B. STAT4 is a target of the hematopoietic zinc-finger transcription factor Ikaros in T cells. FEBS Lett 2005;579:4470–8.
24. Trinh LA, Ferrini R, Cobb BS, Weinmann AS, Hahm K, Ernst P, et al. Down-regulation of TDT transcription in CD4(+)CD8(+) thymocytes by Ikaros proteins in direct competition with an Ets activator. Genes Dev 2001;15:1817–32.
25. Wu C, Sun M, Liu L, Zhou GW. The function of the protein tyrosine phosphatase SHP-1 in cancer. Gene 2003;306:1–12.
26. Nakamura T, Jenkins NA, Copeland NG. Identification of a new family of Pbx-related homeobox genes. Oncogene 1996;13: 2235–42.
27. Peng DF, Razvi M, Chen H, Washington K, Roessner A, Schneider-Stock R, et al. DNA hypermethylation regulates the expression of members of the Mu-class glutathione S-transferases and glutathione peroxidases in Barrett's adenocarcinoma. Gut 2009; 58:5–15.
28. Koipally J, Renold A, Kim J, Georgopoulos K. Repression by Ikaros and Aiolos is mediated through histone deacetylase complexes. EMBO J 1999;18:3090–100.